	Form Approved OMB NO. 0704-0188

1. AGENCY USE ONLY (Leave Blank)	2. REPORT DATE	3. REPORT TYPE AND DATES COVERED

4. TITLE AND SUBTITLE	5. FUNDING NUMBERS
Kinetics of the NH Reaction with H2 and Reassessment of HNO Formation from NH + CO2, H2O	DAAD19-03-1-0046
6. AUTHOR(S) See Attached	
7. PERFORMING ORGANIZATION NAME(S) AND ADDRESS(ES) Rensselaer Polytechnic Institute	8. PERFORMING ORGANIZATION REPORT NUMBER
9. SPONSORING / MONITORING AGENCY NAME(S) AND ADDRESS(ES) U. S. Army Research Office P.O. Box 12211 Research Triangle Park, NC 27709-2211	10. SPONSORING / MONITORING AGENCY REPORT NUMBER 43081.4-CH

11. SUPPLEMENTARY NOTES

The views, opinions and/or findings contained in this report are those of the author(s) and should not be construed as an official Department of the Army position, policy or decision, unless so designated by other documentation.

12 a. DISTRIBUTION / AVAILABILITY STATEMENT	12 b. DISTRIBUTION CODE
Approved for public release; Federal Purpose Rights	

13. ABSTRACT (Maximum 200 words)

See attached

14. SUBJECT TERMS	15. NUMBER OF PAGES
	16. PRICE CODE

17. SECURITY CLASSIFICATION OR REPORT	18. SECURITY CLASSIFICATION *ON THIS PAGE*	19. SECURITY CLASSIFICATION *OF ABSTRACT*	20. LIMITATION OF ABSTRACT
UNCLASSIFIED	**UNCLASSIFIED**	**UNCLASSIFIED**	UU

NSN 7540-01-280-5500

Standard Form 298 (Rev.2-89)
Prescribed by ANSI Std. 239-18
298-102

Available online at www.sciencedirect.com
SCIENCE DIRECT
ELSEVIER
Combustion and Flame 145 (2006) 543–551
Combustion and Flame
www.elsevier.com/locate/combustflame

Kinetics of the NH reaction with H_2 and reassessment of HNO formation from NH + CO_2, H_2O

Arthur Fontijn [a,*], Sayed M. Shamsuddin [a,1], Duane Crammond [a,✠], Paul Marshall [b,*], William R. Anderson [c,*]

[a] *High-Temperature Reaction-Kinetics Laboratory, The Isermann Department of Chemical and Biological Engineering, Rensselaer Polytechnic Institute, Troy, NY 12180-3590, USA*
[b] *Department of Chemistry, University of North Texas, P.O. Box 305070, Denton, TX 76203-5070, USA*
[c] *AMSRD-ARL-WM-BD, U.S. Army Research Laboratory, Aberdeen Proving Ground, MD 21005-5069, USA*

Received 12 July 2005; received in revised form 20 December 2005; accepted 26 December 2005
Available online 7 February 2006

Abstract

The reaction of ground-state NH with H_2 has been studied in a high-temperature photochemistry (HTP) reactor. The NH($X^3\Sigma$) radicals were generated by the 2-photon 193 nm photolysis of NH_3, following the decay of the originally produced NH($A^3\Pi$) radicals. Laser-induced fluorescence on the NH($A^3\Pi$–$X^3\Sigma$ 0,0) transition at 336 nm was used to monitor the progress of the reaction. We obtained k (833–1432 K) = $3.5 \times 10^{-11}\exp(-7758\ \mathrm{K}/T)$ $\mathrm{cm^3\,molecule^{-1}\,s^{-1}}$, with $\pm 2\sigma$ precision limits varying from 12 to 33% and corresponding accuracy levels from 23 to 39%. This result is in excellent agreement with that of Rohrig and Wagner [Proc. Combust. Inst. 25 (1994) 975] and the data sets can be combined to yield k (833–1685 K) = $4.4 \times 10^{-11}\exp(-8142\ \mathrm{K}/T)$. Starting with this agreement, it is argued that their rate coefficients for NH + CO_2 could not be significantly in error [Proc. Combust. Inst. 25 (1994) 975]. This, combined with models of several combustion systems, indicates that HNO + CO cannot be the products, contrary to their suggestion [Proc. Combust. Inst. 25 (1994) 975]. Ab initio calculations have been performed which confirm this conclusion by showing the barriers leading to these products to be too high compared to the measured activation energies. The calculations indicate the likelihood of formation of adducts, of low stability. These then may undergo further reactions. The NH + H_2O reaction is briefly discussed and it is similarly argued that HNO + H_2 cannot be the products, as had been previously suggested.

Keywords: NH; HNO; High temperature; Photochemistry reactor; Propellant dark zones; Rate coefficients; Kinetics models; Ab initio calculations

* Corresponding authors.
E-mail addresses: fontia@rpi.edu (A. Fontijn), marshall@unt.edu (P. Marshall), willie@arl.army.mil (W.R. Anderson).
[1] On leave from Department of Applied Chemistry and Chemical Technology, University of Dhaka, Dhaka 1000, Bangladesh.
✠ Deceased.

0010-2180/$ – see front matter
doi:10.1016/j.combustflame.2005.12.012

1. Introduction

Knowledge of the kinetics of reactions of, or leading to, NH is important in combustion research. For the title reactions, apparently the only direct observations are those of Rohrig and Wagner, who studied these reactions within the 1100–2000 K temperature range behind shock waves [1]. NH in its ground electronic state ($X^3\Sigma$) was produced by thermal dissociation of HN_3. Its concentration was monitored by cw laser absorption. For the reaction

$$NH(X^3\Sigma) + H_2(X^1\Sigma) \rightarrow NH_2(X^2B) + H(^2S),$$
$$\Delta H^0_{298} = 50 \pm 2\ \text{kJ mol}^{-1} \quad (1)$$

they obtained k_1 (1156–1685 K) = $(1.7 \pm 0.8) \times 10^{-10} \exp(-10{,}100 \pm 200)\ \text{K}/T$), for

$$NH(X^3\Sigma) + CO_2(X^1\Sigma) \rightarrow HNO(X^1A) + CO(X^1\Sigma),$$
$$\Delta H^0_{298} = 33 \pm 3\ \text{kJ mol}^{-1} \quad (2)$$

they determined k_2 (1201–1912 K) = $(1.7 \pm 0.8) \times 10^{-11} \exp(-7220 \pm 200)\ \text{K}/T$), and for

$$NH(X^3\Sigma) + H_2O(X^1A) \rightarrow HNO(X^1A) + H_2(X^1\Sigma),$$
$$\Delta H^0_{298} = -8 \pm 3\ \text{kJ mol}^{-1} \quad (3)$$

they measured k_3 (1329–1906 K) = $(3.3 \pm 1.6) \times 10^{-11} \exp(-6970 \pm 200\ \text{K}/T)$. Here the rate coefficients are expressed in $\text{cm}^3\ \text{molecule}^{-1}\ \text{s}^{-1}$. The heats of formation are taken from the JANAF tables [2], except for NH, NH_2, and HNO, which are from Anderson [3,4].

For reaction (2), Rohrig and Wagner concluded that HNO + CO are the products of the CO_2 reaction, as all other product channels they considered are too endothermic in view of the observed activation energy. For reaction (3), they identified several other energetically accessible channels, but considered the products shown as the most likely. There are, however, several difficulties with these conclusions. When either or both of the reverse reactions (−2) or (−3) with $k_{-2}(T)$ and $k_{-3}(T)$ determined from the above expression and the thermochemistry are used in models of several combustion systems, global reaction rates are too fast by one to four orders of magnitude; detailed analysis revealed in all cases that the problem is intimately connected to the inclusion of these reverse processes. These models include: (i) that of Glarborg et al. [5] for NO reduction in rich NO/CO/H_2 mixtures, in two flow reactors, for the 1200 to 1800 K temperature domain, (ii) that of Dagaut et al. [6] for such mixtures in a jet-stirred reactor from 800 to 1400 K, and (iii) Anderson's calculations of the Diau et al. [7] results on the thermal reduction of NO by H_2 in mixtures of these compounds with CO in a static reactor from 900 to 1225 K (see Appendix A). Models for the thickness of dark zones in nitrate ester propellants combustion are similarly very adversely affected [8]. All these groups achieved good comparisons of models with experiments without reactions (−2) and (−3), suggesting that the products and/or rate coefficients are incorrect, and thus decided to omit them and their assumed reverse processes.

It thus appears that either the reported rate coefficients are incorrect or that the products of the NH reactions with CO_2 and H_2O are not those indicated by Eqs. (2) and (3). In order to decide between these possibilities we have now studied one of their reactions [1], i.e., that with H_2, by a very different experimental technique, and have made an ab initio study of reaction (2). The results indicate that HNO + CO and HNO + H_2 are not the products of reactions (2) and (3), respectively. Much further work will be necessary to identify the actual product channels.

2. The NH + H_2 reaction

2.1. Experimental technique

A schematic of the HTP reactor used is shown in Fig. 1. It and the data acquisition procedures have been described frequently [9,10]. Briefly, the 5 cm i.d., 30 cm long ceramic reaction tube is surrounded by resistance heating elements and insulation in a stainless-steel vacuum chamber. The bottom (upstream) plate contains an inlet for N_2 bath gas and a water-cooled inlet through which the photolyte NH_3 and the second reactant gas, here H_2, flow separately. Teledyne–Hastings mass-flow controllers are used, and pressure is measured with an MKS Baratron transducer. The linear gas velocities, $\bar{v}$, are fast enough to provide each photolysis pulse with a fresh reaction mixture. Residence times between the cooled inlet and the observed reaction zone are long compared to the reaction times and are chosen such that mixing is at least 99% complete [11,12].

The reactor contains four side ports at right angles. Two facing ports have Brewster angle windows through one of which the 193 nm photolysis laser radiation (Lambda Physik Compex 201) is introduced. The other window provides the entrance port for the collinear diagnostic beam from a Lambda Physik LPX 100 excimer FL 3002 dye laser combination. The photolysis radiation can be focused on the center of the reaction tube with a plano-convex lens. The dye laser is tuned to 336 nm to pump the

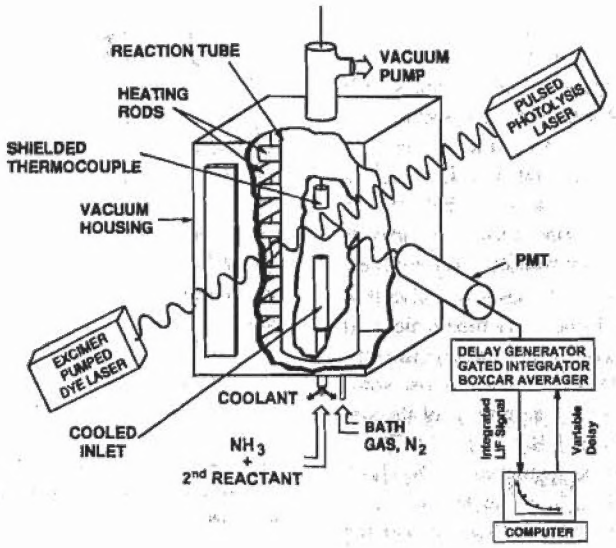

Fig. 1. Schematic of the HTP reactor.

Table 1
Summary of the rate coefficient measurements of the $NH(X^3\Sigma) + H_2 \rightarrow NH_2 + H$ reaction

T (K)	P (mbar)	[M] (10^{18} cm^{-3})	$[H_2]_{max}$ (10^{16} cm^{-3})	LP (mJ)	$[NH_3]$ (10^{14} cm^{-3})	z (cm)	$\bar{v}$ (cm s^{-1})	$(k_i \pm \sigma_{ki})$ (10^{-14} cm^3 molecule^{-1} s^{-1})
833	138	1.20	9.71	75	5.37	12	23.1	0.47 ± 0.11
869	219	1.82	6.35	81	9.43	16	14.9	0.30 ± 0.23
934	305	2.36	15.40	111	6.90	12	11.5	0.69 ± 0.14
978	181	1.34	12.20	24	5.05	12	21.2	1.07 ± 0.17
1025	138	0.97	8.08	66	4.25	12	28.4	2.16 ± 0.35
1045	162	1.13	7.40	93	5.00	8	24.2	2.68 ± 0.21
1113	313	2.04	13.10	101	5.96	12	13.3	3.38 ± 0.53
1155	163	1.02	7.47	102	3.00	8	26.4	3.55 ± 0.92
1174	144	0.89	2.65	90	2.73	16	30.2	2.96 ± 0.33
1265	173	0.82	5.28	60	3.30	12	33.3	10.60 ± 1.20
1368	278	1.47	6.93	108	6.67	8	18.1	11.90 ± 1.30
1432	72	0.36	2.11	123	1.57	12	74.2	16.60 ± 2.80

$NH(A^3\Pi - X^3\Sigma\ 0,0)$ transition. The resulting fluorescence is observed with an EMI 9813 QA photomultiplier tube. The PMT signal is processed with Stanford Research SR 250 boxcar integrators, which provide a range of delay times from the photolysis pulse.

The experiments were carried out under pseudo-first-order conditions, with $[NH] \ll [H_2] \ll [N_2]$. Under these conditions, the fluorescence intensity I, which is proportional to [NH], is expressed by

$$I = I_0 \exp(-k_{ps1} t) + B. \quad (4)$$

Here k_{ps1} is the pseudo-first-order rate coefficient, $I_0 + B$ is the intensity at time $t = 0$, and B is the background, due mainly to scattered light. The values of k_{ps1} were obtained by a weighted fit of the observed I vs t profiles to Eq. (4) [13]. Typically, five k_{ps1} measurements at varying $[H_2]$ were used to obtain the bimolecular rate coefficients, k_i, at the temperature and pressure of the experiment. The minimum $[H_2]$ values were set ca. 5 times lower than the maximum values listed in Table 1. The exponentiality of the I vs t plots was tested by a two-stage residual analysis [14]. The analysis consists of a visual inspection of the residual plot followed by the runs test. A new objective validation method, based on the combination of the χ^2 goodness-of-fit and bootstrap (similar to the Monte Carlo) method, is also used [15]. The two methods have been found to be nearly always in agreement.

The gases used were N_2 (99.995% from the liquid) and NH_3 (99.995%) from Praxair and H_2 (99.999%) from Matheson. The H_2 was dried by passing through drierite. The NH_3 was used as 0.3% NH_3 in N_2, premixed in the laboratory.

2.2. NH production

There are a variety of means of producing NH in the literature, most of which are not suitable for photolysis experiments at or near combustion temperatures. The method developed here is based on the observation, by Kenner et al. [16], that 193 nm two-photon photolysis of NH_3 proceeds in part as $NH_3 + h\upsilon \rightarrow NH_2^* + H$ followed by $NH_2^* + h\upsilon \rightarrow NH(A^3\Pi) + H$. The $NH(A^3\Pi)$ has a radiative lifetime of 4.2×10^{-7} s [17]. Hence, on a time scale short compared to the $\geqslant 10^{-4}$ s of the present experiments, the photolysis leads to $NH(X^3\Sigma)$. There is also some direct formation of $NH(X^3\Sigma)$, as well as of the singlet states $NH(a^1\Delta)$ and of $NH(b^1\Sigma)$ [18]. The a state has been shown to be quenched by N_2 [19], k_Q (300 K) = (6–9) $\times 10^{-14}$ cm^3 molecule^{-1} s^{-1}, which was therefore used as the bath gas and as the NH_3 diluent. The highest NH fluorescence intensities were obtained by slightly defocusing the photolysis laser beam. Apparently this reduced photolysis of NH.

2.3. Results and discussion

The measured rate coefficients, and the conditions under which they were obtained, are given in Table 1. To verify that the rate coefficients are independent of the reaction parameters, plots of residuals $[k(T) - k_i]/k(T)$ versus these parameters were prepared. Here $k(T)$ represents the rate coefficients obtained from the fit expression Eq. (5) below, and k_i are the individual rate coefficients measured. The parameters thus checked are as follows: P, total pressure; [M], the corresponding total gas concentration; the second reactant and photolyte concentration; LP, the photolysis laser power; z, the cooled inlet to observation plane distance; $\bar{v}$, the average gas velocity; the corresponding residence time t; the products $LP[H_2]$ and $LP[NH_3]$, and T^{-1}. These residual plots are found to be independent of these parameters.

Fig. 2 shows the present data. These may be fitted by the Marquardt algorithm [20] to the form $A\exp(-E_A/T)$, where σ_{k_i} and $\sigma_T/T = \pm 2\%$ contribute to the weighting of each point. The fitted expression is

$$k_1\ (833\text{–}1432\ \text{K}) = 3.49 \times 10^{-11} \exp(-7758\ \text{K}/T)\ \text{cm}^3\ \text{molecule}^{-1}\ \text{s}^{-1}. \quad (5)$$

The variances and covariances are $\sigma_A^2 = 1.8332 \times 10^{-1}$ A^2, $\sigma_E^2 = 2.3096 \times 10^5$, and $\sigma_{AE}^2 = 203.6$ A. The resulting 2σ precision levels of the fit are between ±12 and ±33%. Allowing liberally for ±20% systematic errors yields accuracy levels from ±23 to ±39%.

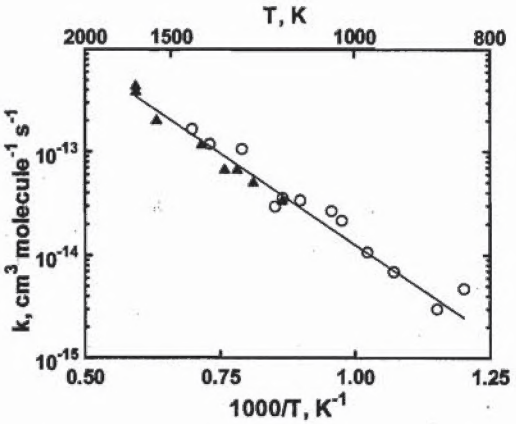

Fig. 2. Arrhenius plot of the NH + H_2 rate coefficients. (○) k, present work; (▲) k, Rohrig and Wagner [1]; (—) best fit to all data, Eq. (6).

Also shown in Fig. 2 are the 1156–1685 K data from Rohrig and Wagner for this reaction. The agreement is very good so that the two data sets can be combined. This yields

$$k_1\ (833\text{–}1685\ \text{K}) = 4.34 \times 10^{-11} \exp(-8142\ \text{K}/T)\ \text{cm}^3\ \text{molecule}^{-1}\ \text{s}^{-1}. \quad (6)$$

Those authors also noted fair agreement with k_1 and k_{-1} data obtained by fitting observations in more complex environments, i.e., for reaction (1) in the 2600–2800 K range [21] and from the reverse reaction [22,23] also at higher temperatures.

3. The NH + CO_2 reaction

3.1. The rate coefficients

The fact that two very different techniques (HTP and shock tube) using different NH production methods (NH_3 photolysis and HN_3 thermal dissociation) yield such excellent agreement for $k_1(T)$ makes it unlikely that there can be a basic error in the technique used for the Rohrig and Wagner measurements on reaction (2). It should be considered if other processes could have significantly influenced their NH– consumption measurements. Conceivably, O atoms from CO_2 dissociation could have interfered due to the very fast reaction of O with NH, leading to NO + H and OH + N, for which the rate coefficients are near the gas kinetic collision rate coefficients, i.e., on the order of 1×10^{-10} cm^3 molecule^{-1} s^{-1}, essentially independent of temperature in the range of interest [24]. However, extrapolated CO_2 dissociation data [25] down to 1912 K indicate the [O] to be too small by several orders of magnitude to have influenced their results [1]. For an impurity to have caused

the measured rates, these would have to have been introduced with the CO_2, as the comparison above for the H_2 reaction suggests no such effect on those experiments. The purity of their CO_2 was 99.995% [1]. Hence any impurity from that source could only have led to reactions at rates orders of magnitude smaller than those observed.

We also examined Rohrig and Wagner's data analysis using the detailed mechanism and technique, described briefly in Appendix A. To this mechanism we added reaction (2) and $k_2(T)$ from their work, and reactions for the HN_3 pyrolysis chemistry, namely

$$HN_3 + M \rightarrow NH + N_2 + M,$$
$$k = 1.2 \times 10^{-9} \exp(-18{,}042\ \mathrm{K}/T)\ [26], \quad (7)$$
$$HN_3 + H \rightarrow NH_2 + N_2,$$
$$k = 3 \times 10^{-11} \exp(-2315\ \mathrm{K}/T)\ [27], \quad (8)$$
$$HN_3 + OH \rightarrow HNOH + N_2, \quad k = 3 \times 10^{-11}, \quad (9)$$
$$HN_3 + NH \rightarrow NH_2 + N_3, \quad k = 2 \times 10^{-11}, \quad (10)$$
$$HN_3 + NH \rightarrow N_2H_2 + N_2, \quad k = 2 \times 10^{-11}. \quad (11)$$

All these ks are in cm^3 $molecule^{-1}$ s^{-1}. The values of Eqs. (9)–(11) are estimates. Within their quoted error limits [1], no influence on $k_2(T)$ was found from these other reactions. In addition, we considered whether H_2O present as contaminant in the shock tube could have affected results. This appears to be the most likely possible contaminant. For this purpose, 1000 ppm H_2O were added to the modeled mixtures. Note that this is probably at least a factor of 100 larger than one would likely encounter in such shock-tube experiments [28]. The effect of the added H_2O is negligible.

Thus, since the $k_2(T)$ data appear substantiated, the assignment of the reaction products as HNO + CO is the most likely cause of the discrepancy between the results of Ref. [1] and the combustion modeling studies noted in the Introduction. To investigate this further, ab initio studies have been performed (see below). It may also be noted that we attempted to measure $k_2(T)$ by the same technique as used for $k_1(T)$. However, in this case O atoms were found to be produced in the photolysis process. These could interfere, and therefore this approach was not pursued further.

3.2. Ab initio calculations and discussion

Reactants, products, transition states, and potential intermediates were characterized with the GAUSSIAN 98 program suite [29]. First, geometries and vibrational frequencies were derived at the B3LYP level of hybrid density functional theory, using the 6-311G(d, p) atomic basis set. Second, single-point energies were obtained by approximate extrapolation of coupled-cluster theory to the complete basis set limit, via application of the CBS-QB3 approach of Petersson and co-workers [30]. These energies, together with zero-point vibrational and thermal corrections, yield enthalpies relative to the reactants, $^3NH + CO_2$, at 298 K.

Some of the ab initio results are summarized in Figs. 3 and 4; complete structural details are given in the Supplementary material. Table 2 lists the CBS-QB3 enthalpies at 298 K and the enthalpies relative to reactants for all adduct species found; these adducts are shown in Fig. 4. The first 7 structures are singlet molecules; CIS/6-311G(d, p) calculations indicate that in each case the lowest triplet energy is higher. Structure 8 of Fig. 4 is a triplet adduct between NH and CO_2.

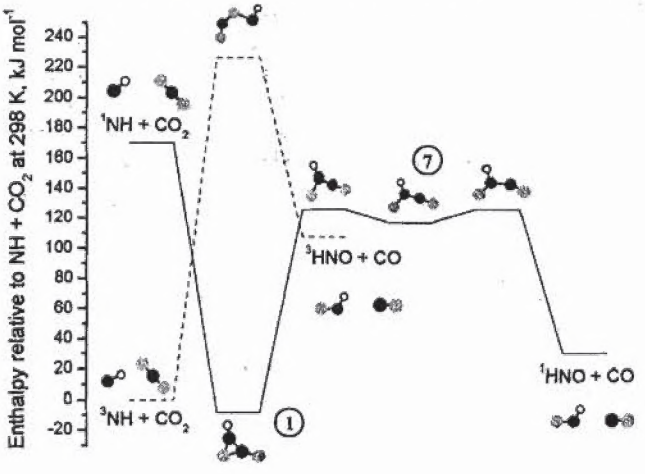

Fig. 3. Potential energy diagram for NH + CO_2 showing paths to HNO + CO. Circled numbers 1 and 7 correspond to those numbers in Table 2 and Fig. 4.

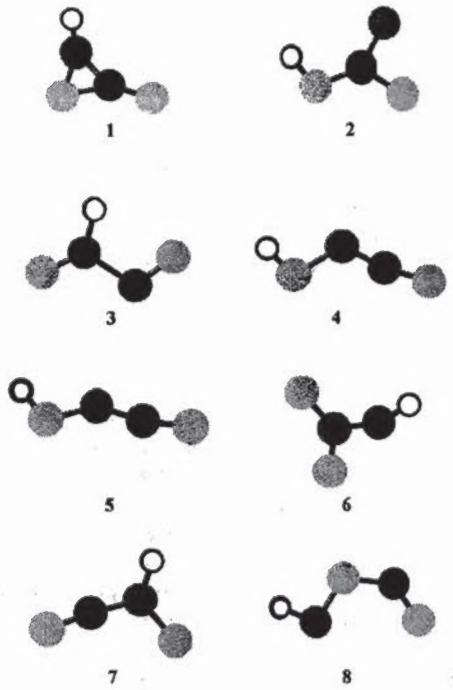

Fig. 4. Various $HNCO_2$ adduct configurations.

Table 2
Ab initio enthalpies for stable $HNCO_2$ species derived via the CBS-QB3 method

Molecule	CBS-QB3 enthalpy at 298 K (au)[a]	Enthalpy relative to $^3NH + CO_2$ at 298 K (kJ mol^{-1})
1	−243.51270	−8
2	−243.48645	61
3	−243.49393	41
4	−243.52232	−33
5	−243.47184	99
6	−243.36024	392
7	−243.46509	117
8	−243.42968	210

[a] 1 au ≈ 2625.5 kJ mol^{-1}.

Fig. 3 shows potential energy diagrams for the reaction of triplet and singlet NH with CO_2. Spin-allowed abstraction to form triplet HNO is possible, but there is a large barrier of 226 kJ mol^{-1}. If intersystem crossing to a singlet surface occurs early in the reaction, then a cyclic adduct, with N attached across a C–O bond, can form, shown as 1 in Figs. 3 and 4. This adduct is too weakly bound, by only 8 kJ mol^{-1} relative to reactants, to be a final sink for ^3NH, but it can undergo further chemistry. The NH group can insert into the C–O bond over a barrier of 126 kJ mol^{-1} to form another adduct, shown as 7 in Figs. 3 and 4. In turn, this second adduct can rearrange while traversing a small barrier and dissociate to $^1HNO + CO$. Both these paths to HNO + CO exhibit major barriers in excess of the endothermicity, and therefore are inconsistent with the measured activation energy, 60 kJ mol^{-1}, corresponding to Eq. (2).

The calculations thus confirm the conclusion from the combined experimental and modeling work that HNO + CO cannot be the products of the $NH + CO_2$ reaction.

An alternative product path is creation of a stable or intermediate adduct. We have tried a variety of initial geometries and from these derived optimized geometries of 8 candidates, which are drawn in Fig. 4. Their enthalpies relative to $^3NH + CO_2$ are summarized in Table 2. The most stable is the HONCO structure 4, but even this is only exothermic by 33 kJ mol^{-1}. It is therefore insufficiently stable to act as a permanent sink for NH at elevated temperatures.

The known thermochemistry in this system provides a check on the accuracy of the ab initio calculations. The overall enthalpy change at 298 K for HNO + CO formation is computed to be 30 kJ mol^{-1}, in accord with the thermochemical value of 33 kJ mol^{-1}. As a second check, the enthalpy change for $^3NH + CO_2 \rightarrow HCN + O_2$ is computed to be 166 kJ mol^{-1}, again in good agreement with the literature-based value [2,3] of 172 kJ mol^{-1}. Computed ΔH^0_{298} values therefore seem to be usefully reliable. An empirical estimate of the singlet-triplet gap in NH is 150 kJ mol^{-1} and prior theoretical work suggests higher values of 157 and 170 kJ mol^{-1} [31]. Degenerate orbitals make ^1NH inappropriate for the single-reference treatments applied here; nevertheless the computed adiabatic singlet-triplet gap of 170 kJ mol^{-1} is close to these prior estimates. In the case of HNO, the singlet-triplet gap is predicted to be 77 kJ mol^{-1}, which is equal to the value derived from a chemiluminescence spectrum [32]. Somewhat lower theoretical values led Gurvich et al. to recommend 72 ± 6 kJ mol^{-1} [33]. The magnitude of this gap makes the spin-allowed path for the NH + CO_2 reaction going to triplet HNO + CO over 100 kJ mol^{-1} endothermic, which is incompatible with the observed activation energies.

4. The $NH + H_2O$ reaction

While we have not explicitly studied this reaction a few remarks about it can be made. Regarding the rate coefficients, one possible concern is that H_2O might have dissociated thermally in the shock experiments. However, calculations based on recommended rate coefficients [34,35] indicate the H_2O dissociation products, H and OH, would have been present in far too small concentrations to have substantially reduced

[NH]. Highly purified H_2O was used [1] and a major impurity effect on the rate coefficients is again highly unlikely. A check of the data analysis of Ref. [1], similar to that performed for the NH + CO_2 reaction above, also showed no significant influence on $k_3(T)$ by other reactions. Thus, the discrepancy with the models can reasonably be attributed to the products not being HNO + H_2. In this case, alternate energetically accessible addition products, H_3NO and H_2NOH, have been suggested [1], but these possibilities need further study.

5. Conclusions

Using an independent technique, the NH + H_2 rate coefficients of Rohrig and Wagner have been confirmed and the temperature range of the observations has been extended. This, and further arguments, leads to the conclusion that their NH + CO_2 and NH + H_2O rate coefficients are also beyond reasonable doubt. However, as discussed in the Introduction and further in Appendix A, modeling of three experiments (Refs. [5,6] and the present modeling of Ref. [7]) and of propellant dark zones is adversely affected if either or both of reactions (2) and (3) and their reverse processes are included in the mechanisms. Detailed analysis indicates in all cases that this is due to the reverse reactions providing a radical source which causes a vast overprediction of the global chemical rates. Excellent results are achieved when these reactions are omitted. These observations thus indicate that the products cannot be HNO + CO or HNO + H_2, respectively.

Furthermore, ab initio calculations of the potential energy surfaces for the NH + CO_2 reaction were performed in the present work. These show that the barriers leading to HNO + CO products are much too high to agree with the activation energy measured in Ref. [1]. The calculations also indicate that adducts can form. These may undergo further reaction. However, since no unique products have been identified, other types of experiments and/or more extensive ab initio calculations are desirable.

Acknowledgments

The work at Rensselaer was supported by the ARO under Grants DAAD 19-03-1-0046 and DAAD 19-99-1-0209. P.M. thanks the NSF (Grant CTS-0113606) and Welch Foundation (Grant B-1174) for support. Computational facilities were provided on the UNT Academic Computing Services' Research Cluster, and by the National Center for Supercomputing Applications (Grant CHE000015N). We thank Dr. P. Glarborg for helpful discussions and him and Dr. P. Dagaut for showing us Ref. [6] before publication and W.F. Flaherty, A. Cosic, and R. Frimpong for assistance with the work. We also acknowledge Drs. A. Fernandez, B. Cosic, and A. Hanf for their active interest during the course of this research.

Appendix A. Significance of reactions (−2) and (−3)

As noted in the Introduction, inclusion of k_{-2} and/or k_{-3} can cause models to strongly deviate from experiments. This may be illustrated by the effect of using k_{-2} or k_{-3} in the model for CO_2 production in NO/H_2/CO mixtures, diluted in Ar, as measured by Diau et al. [7]. The base mechanism used was developed for propellant combustion [8]. It is based on that of Miller and Bowman [36] for nitrogen chemistry in combustion, as further extended in Refs. [37,38]. The modeling utilizes the SENKIN time-dependent, homogeneous gas-phase reaction code [39]. The thermochemistry is taken from Refs. [2–4]. Fig. 5a shows that there is good agreement between the calculated [CO_2] using this base model and the experimental results. Conditions are 0.960 bar, 1000 K, and initial mole fractions of H_2, NO, and CO of 0.0263, 0.0161, and 0.0430, respectively.

Fig. 5b shows the effect of adding HNO + CO → NH + CO_2 to the model, assuming its rate to be determined via the k_2 of Ref. [1] and the thermochemistry. The CO_2 production rate increases by a factor 10^4. Fig. 5c shows the effect of instead adding HNO + H_2 → NH + H_2O to the model, again assuming the rate to be determined via the k_3 of Ref. [1] and the thermochemistry. The CO_2 production rate increases by a factor 10^3. The error becomes cumulatively worse if the two reactions are added together (not shown). Similar erroneous results are obtained for other experimental conditions of Diau et al. Therefore, the actual rates of these two HNO reactions appear to be vanishingly small.

The possibility that an error in the thermodynamics used in reversing reactions (−2) or (−3) might have contributed to the overprediction of the global rate was checked by assuming an error of 20 kJ mol^{-1} in their heats of reaction. This is at least a factor of 5 larger than the error limits in the heats of formation would permit. For the conditions of Fig. 5, the error in either of the computed reverse rate coefficients would be about a factor of 10. Using this factor in the calculation [inputting reactions (2) and (−2) or (3) and (−3) as separate, one-way reactions to CHEMKIN and reducing the rate coefficient for (−2) or (−3)], the time for CO_2 growth is increased (and, thus, the reaction rate decreased) in both cases

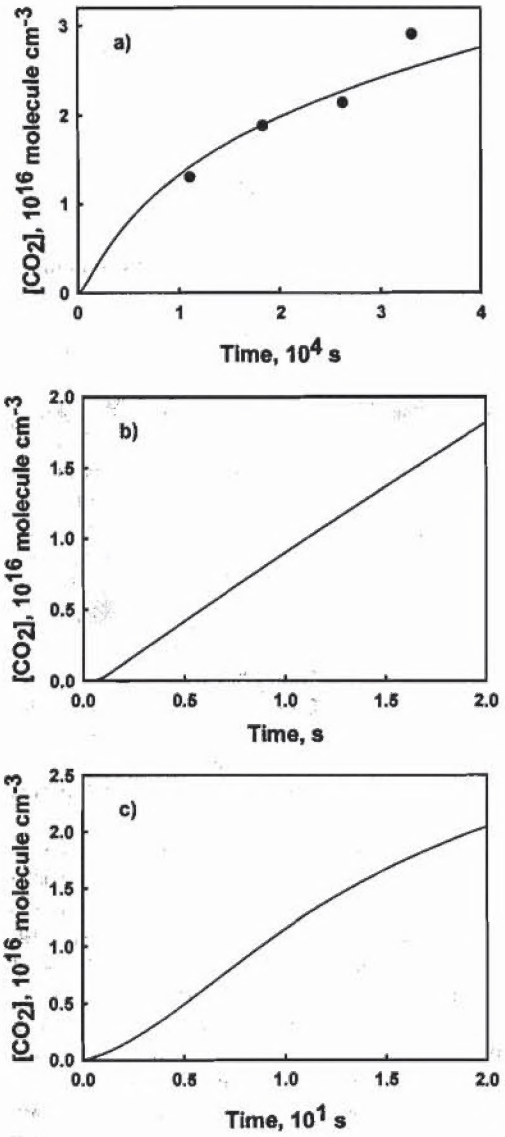

Fig. 5. Influence of the assumed reactions (−2) and (−3). Note the vastly differing time scales of (a)–(c). (a) (●) Experiments from Diau et al. [7]; (—) prediction from the base model. (b) (—) Reaction (−2) added to the model, using k_2 from Rohrig and Wagner [1]. (c) (—) Reaction (−3) added to the model, using k_3 from Rohrig and Wagner [1].

by about a factor of 10. The rate is still far overpredicted.

Supplementary material

Supplementary data for this article may be found in the online version at DOI:10.1016/j.combustflame.2005.12.012. Table 1S lists Cartesian coordinates for the adducts and transition states shown in Figs. 3 and 4, derived at the B3LYP/6-311G(d, p) level of theory.

References

[1] M. Rohrig, H.G. Wagner, Proc. Combust. Inst. 25 (1994) 975.
[2] M.W. Chase, Jr. (Ed.), NIST-JANAF Thermochemical Tables, fourth ed., J. Phys. Chem. Ref. Data, Monograph 9, American Chemical Society, Washington, DC, 1998.
[3] W.R. Anderson, J. Phys. Chem. 93 (1989) 530.
[4] W.R. Anderson, Combust. Flame 117 (1999) 394.
[5] P. Glarborg, P.G. Kristensen, K. Dam-Johanson, M.U. Alzueta, A. Millera, R. Bilbao, Energy Fuels 14 (2000) 828.
[6] P. Dagaut, F. Lecomte, J. Mieritz, P. Glarborg, Int. J. Chem. Kinet. 35 (2003) 564.
[7] E.W. Diau, M.J. Halbgewachs, A.R. Smith, M.C. Lin, Int. J. Chem. Kinet. 27 (1995) 867.
[8] W.R. Anderson, A. Fontijn, in: R.W. Shaw, T.B. Brill, D.L. Thompson (Eds.), Overviews of Recent Research on Energetic Materials, World Scientific, London, 2005, chap. 7.
[9] K. Mahmud, J.-S. Kim, A. Fontijn, J. Phys. Chem. 94 (1990) 2994.
[10] A.S. Narayan, A.G. Slavejkov, A. Fontijn, Proc. Combust. Inst. 24 (1992) 727.
[11] P.S. Riley, B. Cosic, A. Fontijn, Int. J. Chem. Kinet. 35 (2003) 374.
[12] P. Marshall, T. Ko, A. Fontijn, J. Phys. Chem. 93 (1989) 1922.
[13] P. Marshall, Comput. Chem. 11 (1987) 219.
[14] T. Ko, G.Y. Adusei, A. Fontijn, J. Phys. Chem. 95 (1991) 8745.
[15] A. Fernandez, Ph.D. thesis, Rensselaer Polytechnic Institute, Troy, NY, 2002.
[16] R.D. Kenner, F. Rohrer, R.K. Browarzik, A. Kaes, F. Stuhl, Chem. Phys. 118 (1987) 141.
[17] E.C. Chappell, J.B. Jeffries, D. Crosley, J. Chem. Phys. 97 (1992) 2400.
[18] R.D. Kenner, F. Rohrer, F. Stuhl, J. Chem. Phys. 86 (1987) 2036.
[19] K. Yamasaki, S. Okada, M. Koshi, H. Matsui, J. Chem. Phys. 95 (1991) 5087.
[20] W.H. Press, B.P. Flannery, S.A. Teukolsky, W.T. Vetterling, Numerical Recipes, Cambridge Univ. Press, New York, 1986, chap. 14.
[21] J.E. Dove, W.S. Nip, Can. J. Chem. 57 (1979) 689.
[22] D.F. Davidson, K. Kohse-Hoinghaus, A.Y. Chang, R.K. Hanson, Int. J. Chem. Kinet. 22 (1990) 513.
[23] M. Yumura, T. Asaba, Proc. Combust. Inst. 18 (1981) 863.
[24] D.L. Baulch, C.T. Cobos, R.A. Cox, P. Frank, G. Hayman, Th. Just, J.A. Kerr, T. Murrells, M.J. Pilling, J. Troe, R.W. Walker, J. Warnatz, J. Phys. Chem. Ref. Data 23 (1994) 847.
[25] M. Burmeister, P. Roth, AIAA J. 28 (1990) 402.
[26] M. Rohrig, H.G. Wagner, Ber. Bunsen-Ges. Phys. Chem. 98 (1994) 1073.

[27] G. Le Bras, J. Combourieu, Int. J. Chem. Kinet. 5 (1973) 559.
[28] D.F. Davidson, private communication to W.R. Anderson.
[29] M.J. Frisch, G.W. Trucks, H.B. Schlegel, G.E. Scuseria, M.A. Robb, J.R. Cheeseman, V.G. Zakrzewski, J.A. Montgomery Jr., R.E. Stratmann, J.C. Burant, S. Dapprich, J.M. Millam, A.D. Daniels, K.N. Kudin, M.C. Strain, O. Farkas, J. Tomasi, V. Barone, M. Cossi, M.R. Cammi, B. Mennucci, C. Pomelli, C. Adamo, S. Clifford, J. Ochterski, G.A. Petersson, P.Y. Ayala, Q. Cui, K. Morokuma, D.K. Malick, A.D. Rabuck, K. Raghavachari, J.B. Foresman, J. Cioslowski, J.V. Ortiz, A.G. Baboul, B.B. Stefanov, G. Liu, A. Liashenko, P. Piskorz, I. Komaromi, R. Gomperts, D. Martin, J. Fox, T. Keith, M.A. Al-Laham, C.Y. Peng, A. Nanayakkara, M. Challacombe, P.M.W. Gill, B. Johnson, W. Chen, M.W. Wong, J.L. Andres, C. Gonzalez, M. Head-Gordon, E.S. Replogle, J.A. Pople, GAUSSIAN 98, Revision A.9, Gaussian Inc., Pittsburgh, PA, 1998.
[30] J.A. Montgomery Jr., M.J. Frisch, J.W. Ochterski, G.A. Petersson, J. Chem. Phys. 110 (1999) 2822.
[31] K.P. Huber, G. Herzberg, Molecular Spectra and Molecular Structure, IV, Constants of Diatomic Molecules, Van Nostrand–Reinhold, New York, 1979.
[32] T. Ishiwata, H. Akimoto, I. Tanaka, Chem. Phys. Lett. 27 (1974) 260.
[33] L.V. Gurvich, I.V. Veyts, C.B. Alcock, Thermodynamic Properties of Individual Substances, vol. 1, fourth ed., Hemisphere, New York, 1989.
[34] D.L. Baulch, C.J. Cobos, R.A. Cox, P. Frank, Th. Just, J.A. Kerr, M.J. Pilling, J. Troe, R.W. Wacker, J. Warnatz, J. Phys. Chem. Ref. Data 21 (1982) 411.
[35] N. Cohen, K.R. Westberg, J. Phys. Chem. Ref. Data 20 (1991) 1211.
[36] J.A. Miller, C.T. Bowman, Prog. Energy Combust. Sci. 15 (1989) 287.
[37] A. Fontijn, A. Goumri, A. Fernandez, W.R. Anderson, N.E. Meagher, J. Phys. Chem. 104 (2000) 6003.
[38] N.E. Meagher, W.R. Anderson, J. Phys. Chem. 104 (2000) 6013.
[39] A.E. Lutz, R.J. Kee, J.A. Miller, Sandia National Laboratories Technical Report SAND87-8248, October 1988.